Journal of Affective Disorders 309 (2022) 19–26

Contents lists available at ScienceDirect

Journal of Affective Disorders

journal homepage: www.elsevier.com/locate/jad

Research paper

White matter abnormalities in first-episode patients with depersonalization/derealization disorder: A tract-based spatial statistics study

Yanzhe Ning [a,b,1], Nan Song [a,b,1], Hong Zhu [a,b], Sisi Zheng [a,b], Yuan Jia [a,b], Dongqing Yin [a,b], Kuangshi Li [c,*], Hongxiao Jia [a,b,**]

[a] The National Clinical Research Center for Mental Disorders, Beijing Key Laboratory of Mental Disorders, Beijing Anding Hospital, Capital Medical University, Beijing, China
[b] Advanced Innovation Center for Human Brain Protection, Capital Medical University, Beijing, China
[c] Dongzhimen Hospital, Beijing University of Chinese Medicine, Beijing, 100700, China

ARTICLE INFO

Keywords:
Depersonalization / derealization disorder
White matter
TBSS
Cognitive impairment

ABSTRACT

Background: Neuroimaging studies on depersonalization / derealization disorder (DPD) have revealed that there are structural and functional alterations across numerous brain regions. However, to date, the exact white matter abnormalities that are associated with different clinical symptoms and cognitive impairments in first-episode, drug-naïve patients with DPD remain unclear.

Methods: Overall, 25 first-episode, drug-naïve patients with DPD and 23 healthy controls were recruited and underwent DTI scans. The tract-based spatial statistics analysis was conducted in order to determine white matter microstructural changes between the two groups. Correlation analysis was conducted between the fractional anisotropy (FA) of abnormal WM fibers and the total score of the 30-item Cambridge Depersonalization Scale (CDS-30), cognitive assessments.

Results: Patients with DPD demonstrated higher FA in the right corpus callosum (CC), and posterior corona radiate (CR), compared to healthy controls. The FA in the right CC demonstrated a positive correlation with total score of CDS-30, numbing, unreality of self, perceptual alterations, and temporal disintegration, respectively. FA in the right CR region indicated a positive correlation with the total score of CDS-30, unreality of self, perceptual alterations, and temporal disintegration, respectively. Furthermore, FA in the right CR region was found to be negatively correlated with the Continuous Performance Test and the Stroop color-word test.

Conclusion: The altered white matter microstructure and cognitive impairments of medication naïve DPD patients were observed. Abnormalities in the integrity of CC and CR were associated with severity of symptoms and cognitive impairments, which may provide a potential biomarker for clinical studies on DPD.

1. Introduction

Depersonalization / derealization disorder (DPD) is a distressing impairment of self-awareness, and affect around 1%–2% of the general population (Hunter et al., 2004; Michal et al., 2009; Lee et al., 2012), as well as about 5% of psychiatric outpatient samples (Foote et al., 2006). DPD manifests as a feeling of unreality about the self and the world. The high incidence is accompanied by damage to the life and work of patients, including increased suicidal ideation (Michal et al., 2010), elevated symptoms of depression/anxiety (Schlax et al., 2020), and is associated with first-rank symptoms of schizophrenia-spectrum psychoses (Humpston et al., 2020). Although substantial efforts have been

Abbreviations: DPD, depersonalization / derealization disorder; FA, fractional anisotropy; CC, corpus callosum; CR, corona radiate; WM, white matter; TBSS, **tract-based spatial statistics**.

* Corresponding author.
** Correspondence to: H.X., The National Clinical Research Center for Mental Disorders, Beijing Key Laboratory of Mental Disorders, Beijing Anding Hospital, Capital Medical University, Beijing, China.
E-mail addresses: a3376@bucm.edu.cn (K. Li), jhxlj@ccmu.edu.cn (H. Jia).

[1] Yanzhe Ning and Nan Song contributed equally.

https://doi.org/10.1016/j.jad.2022.04.127
Received 28 July 2021; Received in revised form 16 April 2022; Accepted 19 April 2022
Available online 23 April 2022
0165-0327/© 2022 Elsevier B.V. All rights reserved.

made in the field, the neuro-mechanisms of DPD remain unclear.

Magnetic resonance imaging (MRI) is a non-invasive examination method that has opened a window into the brain to explore the neural mechanisms of mental disorders. The different types of MRIs include functional MRI, structural MRI, and diffusion tensor imaging (DTI). Functional and structural MRI studies of DPD have been associated with structural and functional alterations across a variety of distinct brain regions (Sierra et al., 2014; Daniels et al., 2015; Medford et al., 2016; Scalabrini et al., 2020). Nevertheless, only a few DTI studies have been conducted on DPD. DTI, which is a type of special MRI technique, has been widely used in measuring the structural connectivity of white matter (WM) tracts, and provides information on cellular integrity (Radlinska et al., 2010). The fractional anisotropy (FA) is the most widely used in measuring of water movement, and represents the degree of directionality of microstructures, including axons and myelin (Alexander et al., 2007). The FA reduction can be interpreted as axonal demyelination (Bozzali et al., 2012). One recent study on the WM network among patients with DPD demonstrated decreased FA values between the right temporoparietal and left temporal regions compared to healthy controls (HCs) (Sierk et al., 2018). Nonetheless, this study enrolled DPD patients with certain comorbidities or psychotropic medications. Significantly, no study reported structural connectivity of WM in first-episode, drug-naïve patients with DPD. Furthermore, cognitive processing deficits in early perceptual, information processing, attention and executive function have previously been reliably demonstrated among patients with DPD (Guralnik et al., 2007; Guralnik et al., 2000; Lemche et al., 2016). The deficits in attention and concentration are core cognitive symptoms, which patients with DPD frequently experience (Millman et al., 2021). However, the exact abnormalities of WM associated with different clinical symptoms and cognitive impairments in first-episode, drug-naïve patients with DPD still remain unclear.

In the current study, 25 first-episode, drug-naïve patients with DPD and 23 healthy controls were recruited and underwent DTI scans. TBSS is a method that is used for analyzing WM fiber bundles, which has been applied to explore the white matter integrity of mental disorders. TBSS analysis was carried out to detect WM microstructural changes between the two groups. Next, we performed correlation between the FA of abnormal WM fibers and the total score of the 30-item Cambridge Depersonalization Scale (CDS-30), five symptoms (i.e. numbing, unreality of self, perceptual alterations, unreality of surroundings and temporal disintegration) generating from CDS-30, and cognitive assessments on patients with DPD.

2. Methods

This study was granted approval by the Beijing Anding Hospital Ethics Committee. All participants signed written informed consents before inclusion in this study.

2.1. Subjects

Overall, 25 patients (six females) were referred to the Psychiatric Clinic at the Beijing Anding Hospital and were diagnosed with DPD according to the Chinese version of ICD-10 (F48.1) criteria by both experienced psychiatrists and the 30-item Cambridge Depersonalization Scale (CDS-30) >70(Sierra and Berrios, 2000). Additionally, the patients should also meet the criteria below, including first-episode, drug-naïve treatment; aged 18 to 40 years old; right-handed; and provided a signed informed consent form. The exclusion criteria were as follows: a history of anxiety disorder, major depressive disorder or current posttraumatic stress disorder; history of organic pathologic changes; history of drug or alcohol abuse; and any MRI contraindication. Another 23 healthy controls (eight females) were recruited with no history of psychiatric and neurological disorders, were aged 18 to 40 years old and were right-handed.

2.2. Assessments

In order to assess symptom severity of depersonalization and derealization, patients with DPD fulfill the Chinese versions of the CDS-30 prior to the MRI. The Chinese version of CDS-30 was confirmed to have good reliability and validity in community samples in China (Jia et al., 2010). The CDS-30 has comprised five symptoms (i.e. numbing, unreality of self, perceptual alterations, unreality of surroundings and temporal disintegration) that serve as the symptom criteria for a better diagnosis of DPD (Simeon et al., 2008). The Hamilton Anxiety Rating Scale (HAMA) and the Hamilton Depression Scale (HAMD) were utilized to evaluate anxiety and depression, respectively (Goldberger et al., 2011; Hamilton, 1960).

The cognitive tests in our study were chosen, in part from the Chinese version of Measurement and Treatment Research to Improve Cognition in Schizophrenia Consensus Cognitive Battery (MCCB) (Shi et al., 2015). The cognitive assessments lasted one hour and were operated in the following order. First, information processing speed and executive functions were assessed by Trail Making Test versions A and B (TMT). Second, attention and information processing speed were measured by Brief Assessment of Cognition in Schizophrenia: Symbol coding (BACS-SC). Third, verbal learning was measured by the Hopkins Verbal Learning Test (HVLT, Chinese version). Fourth, visual learning was assessed by the Brief Visuospatial Memory Test (BVMT), attention or vigilance assessed by the Continuous Performance Test (CPT). Moreover, the Chinese version of the Stroop color-word test (SCWT) was employed in the current study, which assessed selective attention and executive function (Zhou et al., 2012).

2.3. MRI data acquisition

DTI images were acquired using a 3.0T MRI scanner (Siemens, Prisma, Germany) in the Beijing Anding Hospital. During scanning, each subject's head was immobilized by foam head holders in order to minimize head movements during scanning. Additionally, earplugs were worn throughout the experiment in order to attenuate MRI gradient noise.

Prior to DTI scanning, a standard 3D T1-weight high-resolution structural image was acquired using the following parameters, including voxel size = 1 mm^3, TR = 2530 ms, TE = 3.39 ms, flip angle = 90°, matrix = 256 × 256, field of view = 256 mm × 256 mm, and slice thickness = 1 mm. The DTI data lasted 12 min and 30 s with a single-shot, echo-planar imaging sequence. The diffusion sensitizing gradients were applied along the 64 non-collinear directions (b = 1000 s/mm^2) with an acquisition without diffusion weighting (b = 0 s/mm^2). Furthermore, specific parameters were as follow: TR = 11,000 ms, TE = 98 ms, matrix = 128× 128, field of view = 256 mm × 256 mm, and slice thickness = 2.0 mm with no gap.

2.4. Data processing and analyzing

2.4.1. T1 data processing

Advanced Normalization Tools (ANTs) were utilized to preprocess the T1 data. The T1 images of each subject were initially applied to the bias field correction and were resampled to 4 × 4 × 4 mm^3 resolution. Meanwhile the standard template (OASIS template, https://figshare.com/articles/dataset/ANTs_ANTsR_Brain_Templates/915436) was also resampled to this resolution. Then the processed T1 images were aligned to the OASIS template which was resampled. After, the aligned T1 images were segmented into grey matter and white matter. Finally, standardized T1 images without the skull were obtained.

2.4.2. DTI data processing

FMRIB Software Library (FSL), Diffusion Tensor Imaging Toolkit (DTI-TK) and Analysis of Functional NeuroImage (AFNI) software were largely used for DTI data processing and analysis (Li et al., 2015). Firstly,

self-developed software was applied to reorient the original images that were parallel to anterior-posterior commissure line. The brain extraction toolbox (BET) in FSL was utilized for brain extraction, and the fractional intensity threshold of the BET was adjusted into 0.3. The brain extraction toolbox in FSL was used for brain extraction. Subsequently, the extracted images of each subject were linearly aligned to their respective T1 images. After, the eddy current distortion and head motion were corrected. Next, the b-vectors were rotated according to results from the eddy-correct (Leemans and Jones, 2009). Finally, diffusion tensors were calculated with an AFNI software.

After diffusion tensor images were generated, all diffusion tensor maps were normalized to the IIT3 template using DTI-TK. First, the initial template was bootstrapped from each subject's tensor and the IIT3 mean template image in order to achieve optimal spatial normalization. Secondly, all tensors were affinely registered to the initial template through the use of a similarity metric by the method of Euclidean Distance Squared (EDS). The distances between the adjacent sampling points were 4 mm along x, y and z directions and three consecutive iterations were performed. Thirdly, each subject's tensor after affine registration was deformed and aligned to the initial template in order to improve alignment quality by removing the size or shape differences within the local structures. The number of iterations was chosen as six and the iteration for the registration optimization to stop was 0.002, which was recommended by DTI-TK. Then, a matrix that combines the affine transformation and the deformable transformation was applied to the original tensors. Next, tensors after the above processing were combined in order to produce a final average template with characteristics of all subjects. By following the preceding steps, the FA maps were calculated by the diffusion tensors and also normalized to a standard space (Zhang et al., 2007; Zhang and Arfanakis, 2013; Adluru et al., 2012). Then, a mean FA skeleton of the white matter tracts was also generated from the mean FA image, which was created by the final average template. Each subject's FA image was projected onto the skeleton, for which the threshold was 0.2.

3. Statistical analysis

Ultimately, the permutation-based inference nonparametric statistic was applied for comparison of FA values between patients and health controls. The mean FA skeleton was utilized as a mask, and the nonparametric test was executed with 5000 permutations. The significance threshold was determined to be $P < 0.05$ [two-tailed, Family Wise Error (FWE)] using the threshold-free cluster enhancement (TFCE) (Smith and Nichols, 2009).

The clusters with significant differences were defined as ROI (region of interest) for correlation analysis. As mean FA value of each subject were abnormal distribution, the Spearman correlation analysis was performed between the mean FA value of each patient in the ROI, as well as scores of CDS-30, the cognitive assessment. The significance threshold for the correlations was determined to be $p < 0.05$. The strength of the correlation was determined by p values and R values.

4. Results

4.1. Demographic and clinical features

The demographic and clinical data of all participants are detailed in Table 1. The two groups did not show any significant differences in sex (chi-squared test, $p = 0.412$), age ($p = 0.322$) and education ($p = 0.093$). Compared to HCs, patients with DPD demonstrated significantly lower scores in BACS-SC ($p = 0.001$), HVLT ($p < 0.001$), BVMT ($p = 0.004$), CPT($p < 0.001$) and SCTW($p = 0.011$). Additionally, there were no differences in TMT ($p = 0.354$) between the two groups.

Table 1
Demographics and neuropsychological test scores of patients with DPD and healthy controls.

Items	DPD($n = 25$)	HCs($n = 23$)	χ^2/z/t	P value
Female, n(%)	6(24)	8(34.78)	0.674(χ^2)	0.412
age, median (IQR)	24(6)	25(2)	−0.990 (z)	0.322
education, median (IQR)	14.50(6)	16(0)	−1.681 (z)	0.093
TMT, mean ± S.D.	29.84 ± 7.15	27.96 ± 6.63	0.936(t)	0.354
BACS, mean ± S.D.	56.75 ± 9.80	66.70 ± 8.76	−3.662(t)	0.001
HVLT, mean ± S.D.	8.89 ± 0.80	10.01 ± 1.08	−4.067(t)	<0.001
BVMT, mean ± S.D.	9.51 ± 1.48	10.56 ± 0.81	−3.003(t)	0.004
CPT, median (IQR)	2.96(0.82)	3.68(1.15)	−3.064 (z)	<0.001
SCTW, mean ± S.D.	40.92 ± 8.63	49.00 ± 11.95	−2.667(t)	0.011
CDS-30, mean ± S.D.	162 ± 48.02			
HAMD, mean ± S.D.	10.46 ± 4.25			
HAMA, mean ± S.D.	7.58 ± 3.59			

BACS-SC, brief assessment of cognition in schizophrenia: symbol coding; BVMT, brief visuospatial memory test; CDS-30, 30-item Cambridge depersonalization scale; CPT, continuous performance test; HAMA, Hamilton anxiety rating scale; HAMD, Hamilton depression scale; HVLT, Hopkins verbal learning test; IQR, interquartile range; SCWT, Stroop color-word test; TMT, trail making test; S.D., standard deviation.

4.2. TBSS analysis and correlation analysis between FA and symptom severity

In order to assess symptom severity, patients with DPD were required to fulfill the CDS-30 prior to undergoing the MRI. Any patients with DPD over 70 that did the CDS-30 were recruited to perform the TBSS analysis, which showed significantly higher FA values (FWE corrected, $p < 0.05$) in the right body and genu of corpus callosum (CC), anterior, superior and posterior corona radiate (CR) compared to HCs (Fig. 1, Table 2). Next, we conducted the correlation analysis and found that the FA values in the right CC and CR were both positively correlated with the total score of CDS-30 ($R = 0.7480$, $p < 0.0001$; $R = 0.7523$, $p < 0.0001$). These results are displayed in Fig. 2. Furthermore, we carried out correlation analysis between the abnormal FA values and five symptoms that were generated from CDS-30 respectively (shown in Figs. 3, 4). The FA value in the right CC was positively correlated with numbing ($R = 0.4399$; $p = 0.0278$), unreality of self ($R = 0.6842$; $p = 0.0002$), perceptual alterations (R = 0.4399; $p = 0.0270$), and temporal disintegration ($R = 0.4366$; $p = 0.0291$). Additionally, the FA value in the right CR was shown to be positively correlated with unreality of self ($R = 0.6506$, $p = 0.0004$), perceptual alterations ($R = 0.6481$, $p = 0.0005$), and temporal Disintegration ($R = 0.4692$, $p = 0.0180$).

4.3. Correlation analysis between FA and cognitive assessments

The correlation analysis between abnormal FA values and cognitive assessments was also performed. In the right CR, the FA value was shown to be negatively correlated with CPT ($R = -0.4706$, $p = 0.0176$) and SCWT ($R = -0.539$, $p = 0.005$) (Fig. 5). No other significant correlations between abnormal FA values and cognitive assessments were found.

5. Discussion

In this current study, we focused on WM abnormalities and its relationship with different clinical symptoms and cognitive impairments in first-episode, drug-naïve patients with DPD. Our findings demonstrated increased FA in the body and genu of CC, anterior, superior and

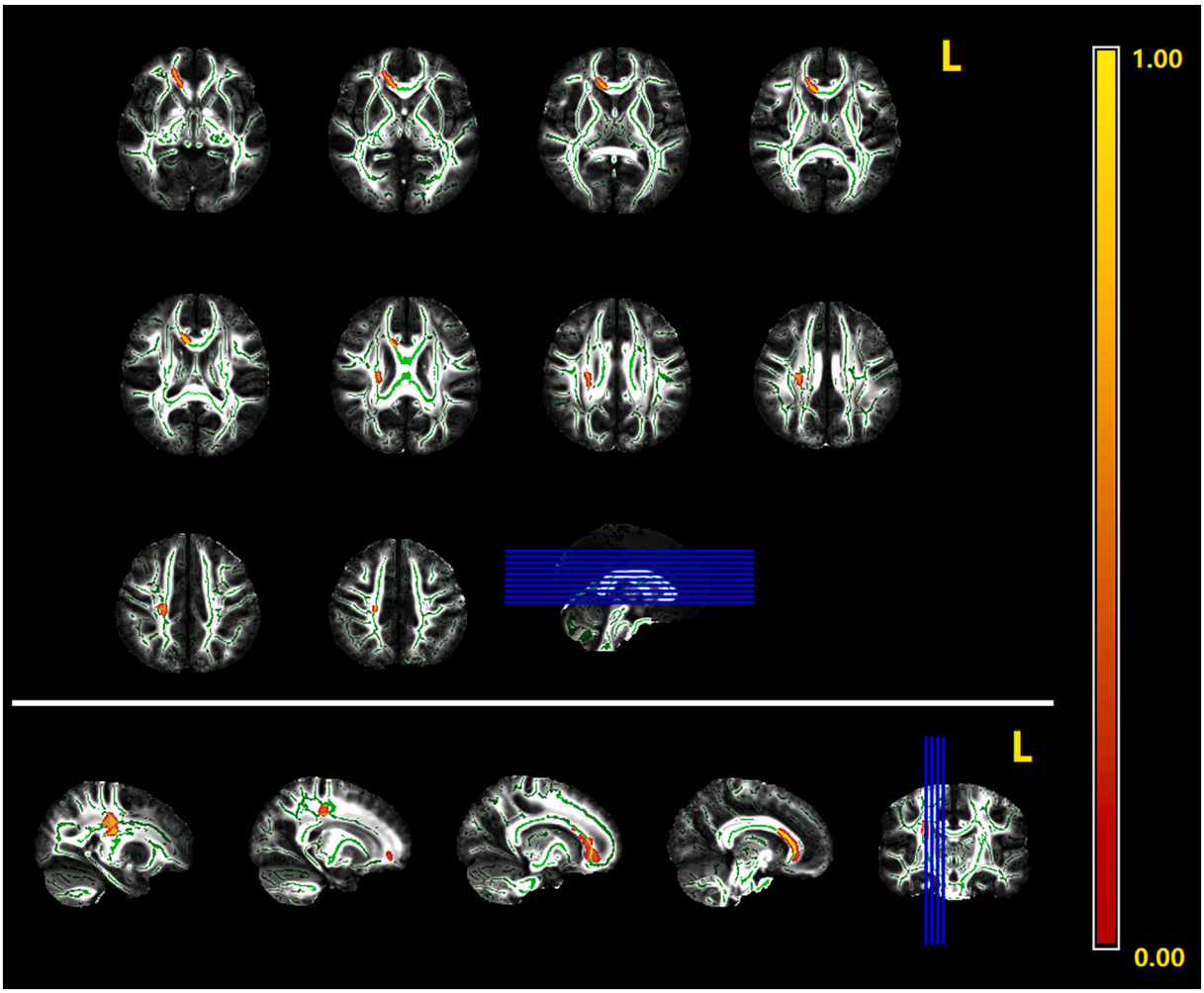

Fig. 1. Group differences between patients with DPD and healthy controls by TBSS analysis. Tract-based spatial statistics analysis of FA volumes revealed higher FA values (in red) when compared with healthy controls. The threshold for the results was set at $P < 0.05$ (threshold-free cluster enhancement corrected). FA, fractional anisotropy; L, left. (For interpretation of the references to color in this figure legend, the reader is referred to the web version of this article.)

Table 2
Group differences of FA values between patients with DPD and healthy controls.

Brain area	Hemisphere	MNI coordinates			*P* value	Voxels number
Genu of corpus callosum	R	16	28	13	0.04	20
Body of corpus callosum	R	10	18	17	0.04	36
Anterior corona radiata	R	17	33	−4	0.04	37
Superior corona radiata	R	21	−24	41	0.03	99
Posterior corona radiata	R	24	−24	23	0.04	6

posterior CR in the right hemisphere among patients with DPD compared to HCs, which were significantly associated with dissociative symptom severity. Furthermore, a wide range of cognitive impairments were discovered and the increased FA value in the right CR was found to be negatively associated with CPT and SCWT.

Herein, we discovered that there was a decline in neuropsychological performances among patients with DPD. Specifically, patients with DPD had impairments in BACS-SC, HVLT, BVMT, CPT and SCWT, which suggests deficits in visual learning and memory, verbal fluency and information processing speed, attention and executive control. These findings are in line with prior studies (Guralnik et al., 2000; Guralnik et al., 2007; Lemche et al., 2016). One recent study on DPD revealed that patients with DPD frequently experienced deficits in attention and concentration (Millman et al., 2021). Hence, according to our results, we postulated that deficits in attention and concentration were the core cognitive impairments of DPD. The impaired cognitive function in the attentional process may be interpreted as disruptions in the sense of familiarity with themselves and surroundings, as well as dissociative experiences (Ozdemir et al., 2015).

The DTI studies on psychiatric disorders mostly demonstrated white matter disruptions with lower FA, as well as significant correlations with clinical scores, which may explain some clinical symptomology (Pasternak et al., 2018). However, high FA in white matter tracts was also detected among patients with some psychiatric disorders. One study among preschool-aged children with ASD demonstrated a significant increase in FA in the CC, corticospinal tract, and six other WM tracts (Andrews et al., 2019). Another meta-analysis study among patients with posttraumatic stress disorder indicated higher FA in the inferior fronto-occipital fasciculus and the left inferior temporal gyrus (Ju et al., 2020). It was worth noting that DTI was a rather approximate technique, and that the FA value is associated with numerous microstructural factors. There are also controversies on the indication of high or low FA values with regards to the degree of structural connectivity (Jones et al., 2013). Interestingly, our current study demonstrated only higher FA in the right CC and CR among patients with DPD compared to healthy

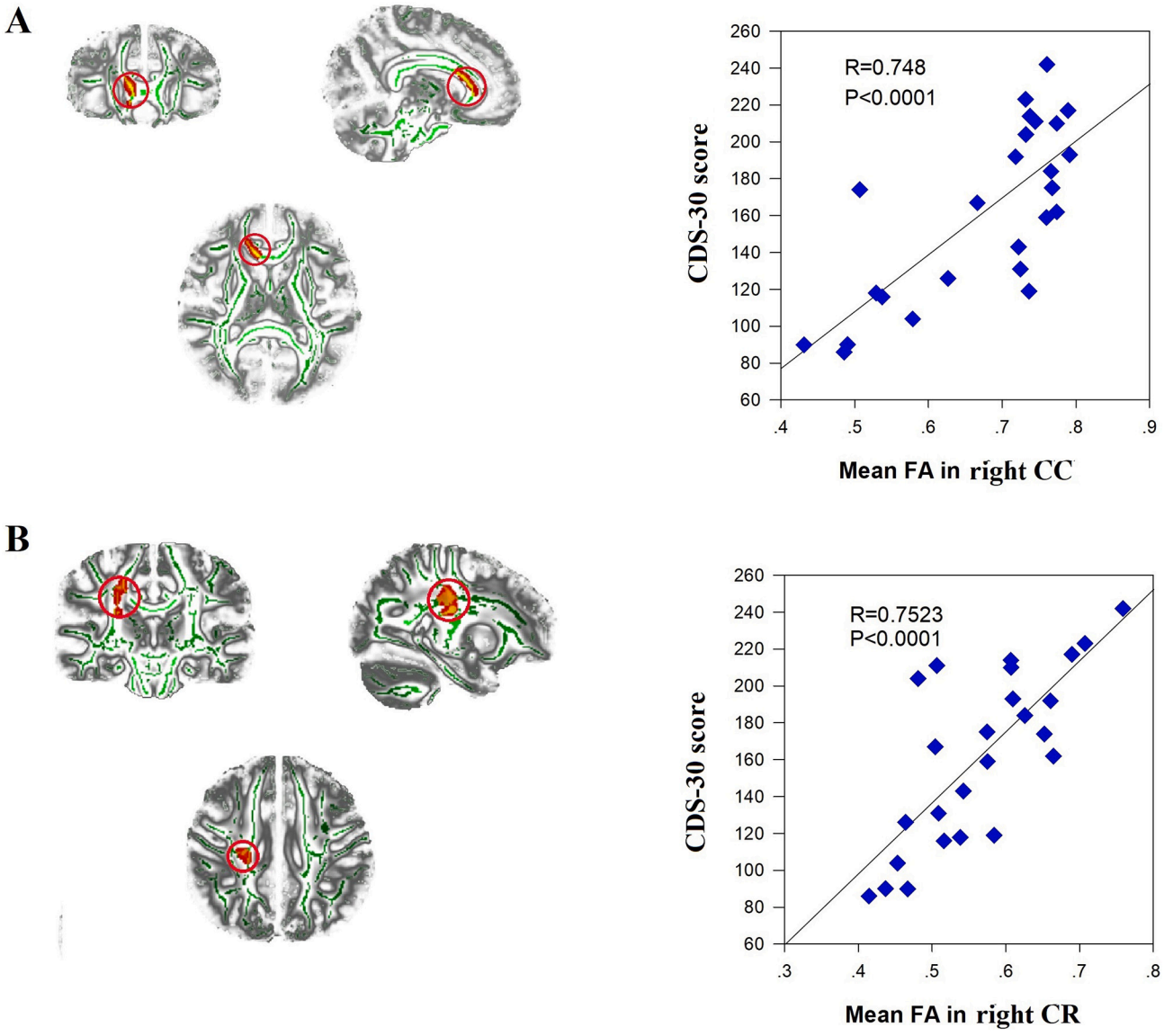

Fig. 2. Correlations between abnormal FA values and CDS-30 scores on patients with DPD.
A, significant positive correlations between the FA values in the right CC and CDS-30 scores. B, significant positive correlations between the FA values in the right CR and CDS-30 scores. CC, corpus callosum; CR, corona radiate; FA, fractional anisotropy.

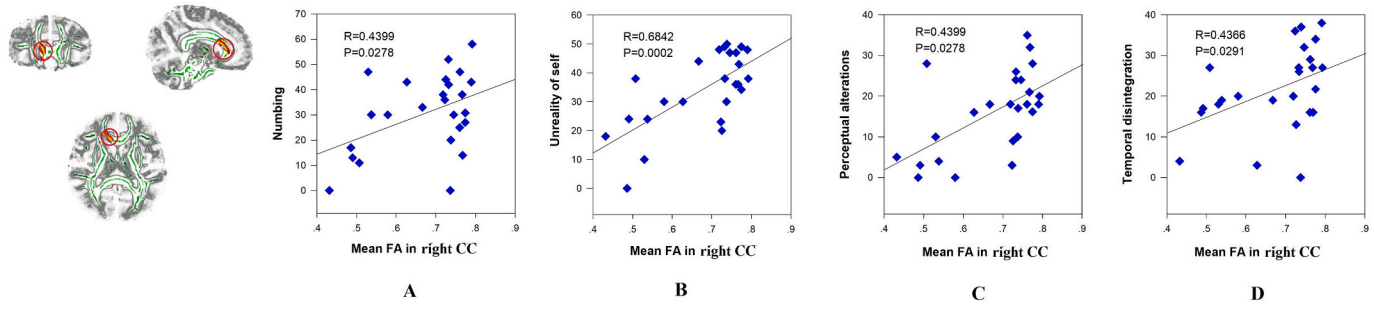

Fig. 3. Correlations between the FA values in the right CC and symptoms.
CC, corpus callosum; FA, fractional anisotropy.

subjects, and a significant correlation with dissociative symptom and cognitive scores, which may be interpreted as pathophysiological abnormalities in the microstructure of patients with DPD.

Our findings demonstrate higher FA in the right CR among patients with DPD, which is positively correlated with dissociative symptom severity. As is known, the CC interconnects both hemispheres with nearly 180 million transcallosal fibers, which monitor interhemispheric integration, as well as control of sensory, motor and cognitive

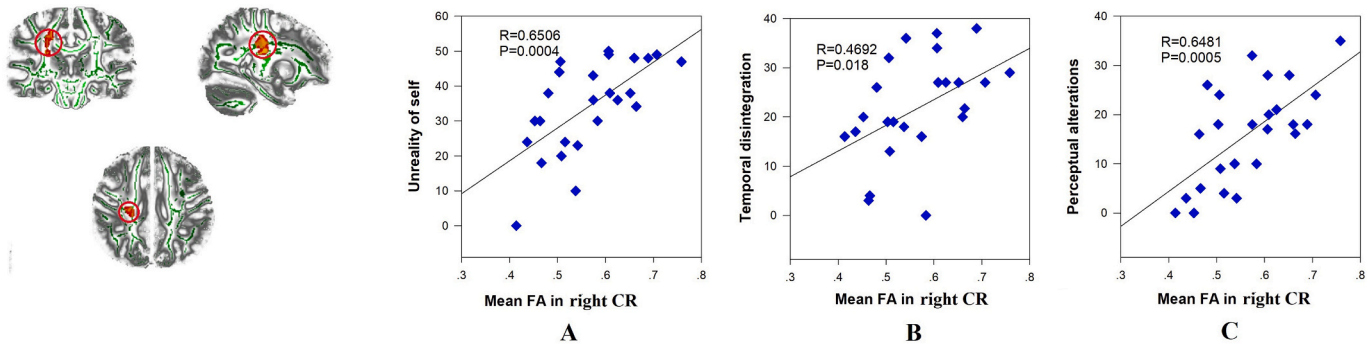

Fig. 4. Correlations between the FA values in the right CR and symptoms.
CR, corona radiate; FA, fractional anisotropy.

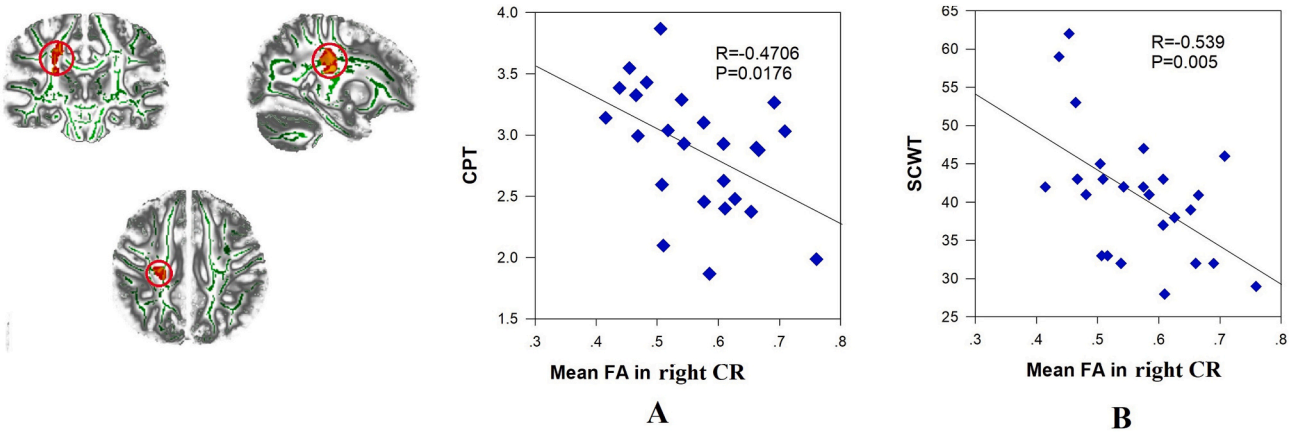

Fig. 5. Correlations between the FA values in the right CR and cognitive assessments on patients with DPD.
CPT, continuous performance test; CR, corona radiate; FA, fractional anisotropy; SCWT, Stroop color-word test.

information (Devinsky and Laff, 2003). The CC mainly projects into the prefrontal, supplementary and primary motor, and sensory areas of the bilateral hemispheres (Hofer and Frahm, 2006). The higher FA in the genu and body of CC suggests abnormal interhemispheric information exchanges between prefrontal lobe and sensory areas, which can interpret cognitive impairments and sensory abnormalities among patients with DPD. The meta-analysis TBSS study on adult obsessive-compulsive disorder revealed that there were changes in FA in the genu and anterior body of CC, which were associated with both emotional and cognitive deficits (Li et al., 2020). Our results also demonstrate positive realtionships between FA in CC and numbing, unreality of self, perceptual alterations, and temporal disintegration. Importantly, one recent study on medication naïve DPD patients showed significantly reduced grey matter volume in the bilateral caudate and thalamus, which was significantly negatively correlated with symptom severity (Daniels et al., 2015). Another white matter network study among patients with DPD indicated higher FA values between the cerebral hemispheres within the left medial orbitofrontal cortex, as well as the right superior frontal gyrus (Sierk et al., 2018). Herein, increased FA in CC indicated a positive association with dissociative symptom severity, and no relationship with anxiety and depressive symptoms. Hence, abnormal FA in CC may partially explain dissociative symptom in DPD.

Patients also indicated relatively higher FA in the right CR, which was positively correlated with dissociative symptom severity, and negatively correlated with CPT and SCWT. As is known, the CR was a WM sheet, which connected cortical area to the subcortical regions, including prefrontal cortex to subcortical nuclei (Axer and Keyserlingk, 2000). Meanwhile, the prefrontal cortices were demonstrated to over-regulate limbic structures, which resulted in emotional numbing on DPD (Sierra and Berrios, 1998). Moreover, CR belongs to the part of frontal-limbic circuitry, which is associated with emotional regulation (Sanjuan et al., 2013). One previous study on DPD revealed that increased dorsal prefrontal cortical activity to emotionally arousing stimuli was associated with the emotional detachment (Lemche et al., 2007). Our results exhibited the positive relationship between FA in CR and dissociative symptoms, including emotional detachment. Hence, the altered FA in CR may explain part of the dissociative symptoms in DPD. The anterior and superior CRs have been demonstrated to be involved in executive control function (Yin et al., 2013; Niogi et al., 2008). Our results indicated a decline in executive ability, as well as the negative relationship between FA values in the CR and SCWT. Patients with DPD frequently report having difficulties in focusing attention. The negative relationship between FA values in the CR and CPT may be interpreted as structural basis of the attention decline among patients with DPD. Altogether, it appears that there is a disrupted microstructure of CR, which may be the potential neuro-mechanism of impaired executive control function and attention in DPD.

However, there are still some limitations in this study. First, as a preliminary and cross-sectional study, it is not clear whether abnormalities in WM fiber were interpreted to be a risk factor for the development of DPD or as a consequence of the disorder. Further longitudinal studies on treatment-related changes in white matter integrity may be needed in the future. Second, it was hard to interpret the high FA. Although the FA result could be explained by dissociative symptoms and cognitive impairments through correlation analysis, there still needs to be further studies on why there is high FA in patients with DPD.

6. Conclusion

In the current study, medication naïve DPD patients demonstrated cognitive impairments. White matter alterations of CC and CR were validated, and were associated with clinical symptoms and cognitive impairments, which may provide potential biomarkers for clinical studies on DPD.

Conflict of Interest

The authors declare there is no conflict of interests and agree to submit the manuscript to the Journal of Affective Disorders. We hereby confirm that we have full access to all aspects of the research and writing process, and we take the final responsibility for the paper.

Acknowledgements

This paper is supported by the National Natural Science Foundation of China (81873398, 81904120), Beijing Hospitals Authority Youth Program (QML20191901, QML20201901), Beijing Hospitals Authority's Ascent Plan (DFL20191901), Beijing Hospitals Authority Clinical Medicine Development of Special Funding (ZYLX202129) and Talents Training Fund of Beijing (2018000021469G292). We would like to thank MogoEdit (https://www.mogoedit.com) for its English editing during the revision of this manuscript.

CRediT authorship contribution statement

Yanzhe Ning and Kuangshi Li made substantial contributions to the conception and design of the work, to the analysis, and interpretation of data, and they drafted the manuscript. Nan Song, Hong Zhu and Sisi Zheng made substantial contributions to the acquisition. Dongqing Yin and Yuan Jia helped draft the manuscript and interpretation of data. Hongxiao Jia approved the final version of the manuscript to be published and agreed to be accountable for all aspects of the work. All authors read, critically revised, and approved the manuscript.

References

Adluru, N., Zhang, H., Fox, A.S., Shelton, S.E., Ennis, C.M., Bartosic, A.M., Oler, J.A., Zakszewski, E., Gee, J.C., Kalin, N.H., Alexander, A.L., Tromp do, P.M., 2012. A diffusion tensor brain template for rhesus macaques. Neuroimage 59, 306–318.
Alexander, A.L., Lee, J.E., Lazar, M., Field, A.S., 2007. Diffusion tensor imaging of the brain. Neurotherapeutics 4, 316–329.
Andrews, D.S., Lee, J.K., Solomon, M., Rogers, S.J., Amaral, D.G., Nordahl, C.W., 2019. A diffusion-weighted imaging tract-based spatial statistics study of autism spectrum disorder in preschool-aged children. J. Neurodev. Disord. 11, 32.
Axer, H., Keyserlingk, D.G., 2000. Mapping of fiber orientation in human internal capsule by means of polarized light and confocal scanning laser microscopy. J. Neurosci. Methods 94, 165–175.
Bozzali, M., Mastropasqua, C., Cercignani, M., Giulietti, G., Bonni, S., Caltagirone, C., Koch, G., 2012. Microstructural damage of the posterior corpus callosum contributes to the clinical severity of neglect. PLoS One 7, e48079.
Daniels, J.K., Gaebler, M., Lamke, J.P., Walter, H., 2015. Grey matter alterations in patients with depersonalization disorder: a voxel-based morphometry study. J. Psychiatry Neurosci. 40, 19–27.
Devinsky, O., Laff, R., 2003. Callosal lesions and behavior: history and modern concepts. Epilepsy Behav. 4, 607–617.
Foote, B., Smolin, Y., Kaplan, M., Legatt, M.E., Lipschitz, D., 2006. Prevalence of dissociative disorders in psychiatric outpatients. Am. J. Psychiatry 163, 623–629.
Goldberger, C., Guelfi, J.D., Sheehan, D.V., 2011. Assessment of anxiety in clinical trials with depressed patients using the Hamilton depression rating scale. Psychopharmacol. Bull. 44, 34–50.
Guralnik, O., Schmeidler, J., Simeon, D., 2000. Feeling unreal: cognitive processes in depersonalization. Am. J. Psychiatry 157, 103–109.
Guralnik, O., Giesbrecht, T., Knutelska, M., Sirroff, B., Simeon, D., 2007. Cognitive functioning in depersonalization disorder. J. Nerv. Ment. Dis. 195, 983–988.
Hamilton, M., 1960. A rating scale for depression. J. Neurol. Neurosurg. Psychiatry 23, 56–62.
Hofer, S., Frahm, J., 2006. Topography of the human corpus callosum revisited–comprehensive fiber tractography using diffusion tensor magnetic resonance imaging. NeuroImage 32, 989–994.
Humpston, C., Harrow, M., Rosen, C., 2020. Behind the opaque curtain: a 20-year longitudinal study of dissociative and first-rank symptoms in schizophrenia-spectrum psychoses, other psychoses and non-psychotic disorders. Schizophr. Res. 223, 319–326.
Hunter, E.C., Sierra, M., David, A.S., 2004. The epidemiology of depersonalisation and derealisation. A systematic review. Soc. Psychiatry Psychiatr. Epidemiol. 39, 9–18.
Jia, X.J., Liu, S.Y., Wang, Z., 2010. Reliability and validity of the Chinese version of the Cambridge personalization scale. J. Neurosci. Ment. Health 10, 551–553.
Jones, D.K., Knosche, T.R., Turner, R., 2013. White matter integrity, fiber count, and other fallacies: the do's and don'ts of diffusion MRI. NeuroImage 73, 239–254.
Ju, Y., Ou, W., Su, J., Averill, C.L., Liu, J., Wang, M., Wang, Z., Zhang, Y., Liu, B., Li, L., Abdallah, C.G., 2020. White matter microstructural alterations in posttraumatic stress disorder: an ROI and whole-brain based meta-analysis. J. Affect. Disord. 266, 655–670.
Lee, W.E., Kwok, C.H., Hunter, E.C., Richards, M., David, A.S., 2012. Prevalence and childhood antecedents of depersonalization syndrome in a UK birth cohort. Soc. Psychiatry Psychiatr. Epidemiol. 47, 253–261.
Leemans, A., Jones, D.K., 2009. The B-matrix must be rotated when correcting for subject motion in DTI data. Magn. Reson. Med. 61, 1336–1349.
Lemche, E., Surguladze, S.A., Giampietro, V.P., Anilkumar, A., Brammer, M.J., Sierra, M., Chitnis, X., Williams, S.C., Gasston, D., Joraschky, P., David, A.S., Phillips, M.L., 2007. Limbic and prefrontal responses to facial emotion expressions in depersonalization. Neuroreport 18, 473–477.
Lemche, E., Sierra-Siegert, M., David, A.S., Phillips, M.L., Gasston, D., Williams, S.C., Giampietro, V.P., 2016. Cognitive load and autonomic response patterns under negative priming demand in depersonalization-derealization disorder. Eur. J. Neurosci. 43, 971–978.
Li, K., Zhang, Y., Ning, Y., Zhang, H., Liu, H., Fu, C., Ren, Y., Zou, Y., 2015. The effects of acupuncture treatment on the right frontoparietal network in migraine without aura patients. J. Headache Pain 16, 518.
Li, Q., Zhao, Y., Huang, Z., Guo, Y., Long, J., Luo, L., You, W., Sweeney, J.A., Li, F., Gong, Q., 2020. Microstructural white matter abnormalities in pediatric and adult obsessive-compulsive disorder: a systematic review and meta-analysis. Brain Behav. 11 (2), e01975.
Medford, N., Sierra, M., Stringaris, A., Giampietro, V., Brammer, M.J., David, A.S., 2016. Emotional experience and awareness of self: functional MRI studies of depersonalization disorder. Front. Psychol. 7, 432.
Michal, M., Wiltink, J., Subic-Wrana, C., Zwerenz, R., Tuin, I., Lichy, M., Brahler, E., Beutel, M.E., 2009. Prevalence, correlates, and predictors of depersonalization experiences in the german general population. J. Nerv. Ment. Dis. 197, 499–506.
Michal, M., Wiltink, J., Till, Y., Wild, P.S., Munzel, T., Blankenberg, S., Beutel, M.E., 2010. Type-D personality and depersonalization are associated with suicidal ideation in the german general population aged 35–74: results from the gutenberg heart study. J. Affect. Disord. 125, 227–233.
Millman, L.S.M., Hunter, E.C.M., Orgs, G., David, A.S., Terhune, D.B., 2021. Symptom variability in depersonalization-derealization disorder: a latent profile analysis. J. Clin. Psychol. 78, 637–655.
Niogi, S.N., Mukherjee, P., Ghajar, J., Johnson, C.E., Kolster, R., Lee, H., Suh, M., Zimmerman, R.D., Manley, G.T., McCandliss, B.D., 2008. Structural dissociation of attentional control and memory in adults with and without mild traumatic brain injury. Brain 131, 3209–3221.
Ozdemir, O., Ozdemir, P.Guzel, Boysan, M., Yilmaz, E., 2015. The relationships between dissociation, attention, and memory dysfunction. Noro Psikiyatr. Ars. 52, 36–41.
Pasternak, O., Kelly, S., Sydnor, V.J., Shenton, M.E., 2018. Advances in microstructural diffusion neuroimaging for psychiatric disorders. NeuroImage 182, 259–282.
Radlinska, B., Ghinani, S., Leppert, I.R., Minuk, J., Pike, G.B., Thiel, A., 2010. Diffusion tensor imaging, permanent pyramidal tract damage, and outcome in subcortical stroke. Neurology 75, 1048–1054.
Sanjuan, P.M., Thoma, R., Claus, E.D., Mays, N., Caprihan, A., 2013. Reduced white matter integrity in the cingulum and anterior corona radiata in posttraumatic stress disorder in male combat veterans: a diffusion tensor imaging study. Psychiatry Res. 214, 260–268.
Scalabrini, A., Mucci, C., Esposito, R., Damiani, S., Northoff, G., 2020. Dissociation as a disorder of integration - on the footsteps of Pierre Janet. Prog. Neuro-Psychopharmacol. Biol. Psychiatry 101, 109928.
Schlax, J., Wiltink, J., Beutel, M.E., Munzel, T., Pfeiffer, N., Wild, P., Blettner, M., Ghaemi Kerahrodi, J., Michal, M., 2020. Symptoms of depersonalization/derealization are independent risk factors for the development or persistence of psychological distress in the general population: Results from the Gutenberg health study. J. Affect. Disord. 273, 41–47.
Shi, C., Kang, L., Yao, S., Ma, Y., Li, T., Liang, Y., Cheng, Z., Xu, Y., Shi, J., Xu, X., Zhang, C., Franklin, D.R., Heaton, R.K., Jin, H., Yu, X., 2015. The MATRICS consensus cognitive battery (MCCB): co-norming and standardization in China. Schizophr. Res. 169, 109–115.
Sierk, A., Daniels, J.K., Manthey, A., Kok, J.G., Leemans, A., Gaebler, M., Lamke, J.P., Kruschwitz, J., Walter, H., 2018. White matter network alterations in patients with depersonalization/derealization disorder. J. Psychiatry Neurosci. 43, 170110.
Sierra, M., Berrios, G.E., 1998. Depersonalization: neurobiological perspectives. Biol. Psychiatry 44, 898–908.
Sierra, M., Berrios, G.E., 2000. The Cambridge depersonalization scale: a new instrument for the measurement of depersonalization. Psychiatry Res. 93, 153–164.
Sierra, M., Nestler, S., Jay, E.L., Ecker, C., Feng, Y., David, A.S., 2014. A structural MRI study of cortical thickness in depersonalisation disorder. Psychiatry Res. 224, 1–7.
Simeon, D., Kozin, D.S., Segal, K., Lerch, B., Dujour, R., Giesbrecht, T., 2008. De-constructing depersonalization: further evidence for symptom clusters. Psychiatry Res. 157, 303–306.

Smith, S.M., Nichols, T.E., 2009. Threshold-free cluster enhancement: addressing problems of smoothing, threshold dependence and localisation in cluster inference. NeuroImage 44, 83–98.
Yin, X., Han, Y., Ge, H., Xu, W., Huang, R., Zhang, D., Xu, J., Fan, L., Pang, Z., Liu, S., 2013. Inferior frontal white matter asymmetry correlates with executive control of attention. Hum. Brain Mapp. 34, 796–813.
Zhang, S., Arfanakis, K., 2013. Role of standardized and study-specific human brain diffusion tensor templates in inter-subject spatial normalization. J. Magn. Reson. Imaging 37, 372–381.
Zhang, H., Avants, B.B., Yushkevich, P.A., Woo, J.H., Wang, S., McCluskey, L.F., Elman, L.B., Melhem, E.R., Gee, J.C., 2007. High-dimensional spatial normalization of diffusion tensor images improves the detection of white matter differences: an example study using amyotrophic lateral sclerosis. IEEE Trans. Med. Imaging 26, 1585–1597.
Zhou, F.C., Xiang, Y.T., Wang, C.Y., Dickerson, F., Au, R.W., Zhou, J.J., Zhou, Y., Shum, D.H., Chiu, H.F., Man, D., Lee, E.H., Yu, X., Chan, R.C., Ungvari, G.S., 2012. Characteristics and clinical correlates of prospective memory performance in first-episode schizophrenia. Schizophr. Res. 135, 34–39.